Splitting of the transition to the antiferroelectric state in $PbZr_{0.95}Ti_{0.05}O_3$ into polar and antiferrodistortive components

F. Cordero,[1] F. Craciun,[1] F. Trequattrini,[2] C. Galassi,[3] P. A. Thomas,[4] D. S. Keeble,[4] and A. M. Glazer[5]

[1]*CNR-ISC, Istituto dei Sistemi Complessi, Area della Ricerca di Roma–Tor Vergata, Via del Fosso del Cavaliere 100, I-00133 Roma, Italy*

[2]*Dipartimento di Fisica, Università di Roma "La Sapienza", P.le A. Moro 2, I-00185 Roma, Italy*

[3]*CNR-ISTEC, Istituto di Scienza e Tecnologia dei Materiali Ceramici, Via Granarolo 64, I-48018 Faenza, Italy*

[4]*Department of Physics, University of Warwick, Coventry CV4 7AL, United Kingdom*

[5]*Department of Physics, Oxford University, Parks Road, Oxford OX1 3PU, United Kingdom*

(Received 31 January 2013; revised manuscript received 26 July 2013; published 27 September 2013)

The phase transformations of ceramic $PbZr_{1-x}Ti_xO_3$ are studied at the composition $x = 0.05$ close to the morphotropic phase boundary between antiferroelectric orthorhombic *Pbam* and ferroelectric rhombohedral phases by elastic, dielectric, and x-ray diffraction measurements. Temperature scans at different rates show that the kinetics of the transition from *R*3*m* to *Pbam* is very sluggish, and is actually split into a slower polar component, appearing in the dielectric susceptibility and a nonpolar component, visible as a sharp stiffening of the Young's modulus. The latter is assigned to the establishment of the oxygen octahedral tilt pattern of the *Pbam* phase, and occurs at once at a temperature that decreases with increasing cooling rate. On heating, the transition occurs at a temperature 65 K higher than on quasistatic cooling, so that both components occur with a faster rate almost together. The Young's modulus presents a variety of apparently different types of anomalies, depending on temperature rate and history, which, however, can be well reproduced in terms of steplike anomalies corresponding to the two components of the *Pbam* $\leftrightarrow$ *R*3*m* transition and the tilt *R*3*c* $\leftrightarrow$ *R*3*m* transition in the region of coexistence of the FE and AFE phases.

DOI: 10.1103/PhysRevB.88.094107 PACS number(s): 77.80.B−, 77.84.Cg, 62.40.+i, 77.22.Ch

I. INTRODUCTION

The ferroelectric perovskite $PbZr_{1-x}Ti_xO_3$ is among the best studied since the main features of its phase diagram were established in the 1950s,[1] but its investigation still provides unexpected results. Besides the polar modes, PZT has unstable rotational degrees of freedom of the O octahedra.[2] The temperatures at which these antiferrodistortive (AFD) tilt modes become unstable never exceed the Curie temperature T_C in PZT, implying that they are less important in determining the physical properties, but the same is not true in other perovskites, notably in the multiferroic $BiFeO_3$,[3] so making the study of the AFD modes and their coupling with the polar ones more than of academic interest. In addition, also in PZT the energetics of the AFD and polar modes become comparable when approaching the $PbZrO_3$ end member, where the temperatures of the two instabilities coincide. Recently, it has been proposed that the merging of tilt and FE transitions occurs already at $x \simeq 0.06$, although no long-range tilt order is established until the lower temperature T_T is reached,[4] and there are even indications of disordered tilting above T_C.[5]

The detection of oxygen octahedral tilting, especially if characterized by short-range order, is not an easy task. In diffraction experiments one has to distinguish it from the effects of cation displacements, which in addition have a stronger scattering cross section for x rays.[6] On the other hand, the uniform susceptibilities are not affected by short correlation lengths, but the dielectric susceptibility contains an overwhelming contribution of the polar modes. Instead, the elastic susceptibility (compliance) is more or less equally affected by AFD and polar modes, so making the combination of elastic, dielectric, and diffraction experiments an effective tool for studying polar and AFD modes, even in the absence of long-range order. In addition, the temperature scans for the elastic and dielectric measurements can be much faster than those for diffraction, so that it is possible to reveal that tilt and polar degrees of freedom at $x = 0.05$ have quite different kinetics.

It is well known that the AFE transition in variously doped $PbZrO_3$ may have extremely large thermal hysteresis and slow kinetics. This has been found in PZT with 5% Ti and doped with Nb[7,8] and La,[9] but also in $Pb_{1-x}Ba_xZrO_3$,[10–12] and explained in terms of charged defects, that stabilize the FE phase over the AFE one. The role of such defects in inducing an intermediate FE phase has been studied also in undoped $PbZrO_3$ crystals,[13] and is found to play a role in the hysteretic behavior of χ even above T_C.[14] At least for $Pb_{1-x}Ba_xZrO_3$, it has been proposed that defects stabilizing the FE phase can be induced by microcracking during the AFE/FE transition, as a consequence of the particularly high volume change involved in the transition.[10]

Here we show that, during cooling, $PbZr_{0.95}Ti_{0.05}O_3$ undergoes a combined AFE and AFD transition from space group *R*3*m* to *Pbam* only in quasistatic conditions, while in normal temperature scans two transitions are found, involving separately the AFD and AFE modes.

II. EXPERIMENTAL

Ceramic samples of $PbZr_{0.95}Ti_{0.05}O_3$ were prepared by the mixed-oxide method in the same manner as a previous series of samples.[15,16] The oxide powders were calcined at 800 °C for 4 h, pressed into bars, sintered at 1250 °C for 2 h, and packed with $PbZrO_3 + 5$ wt% excess ZrO_2 to prevent PbO loss. The powder x-ray diffraction did not reveal any trace of impurity phases. The densities were about 95% of the

theoretical values and the grains were large, with sizes of 5–20 μm. Sample No. 1 was cut as a thin bar 4-cm long and 0.6-mm thick for anelastic and dielectric experiments; sample No. 2, used for XRD, was crushed in an agate mortar from the same sintered block as sample No. 1, and annealed in air for 4 h at 500 °C. To check the reproducibility of the results, sample No. 3 was cut from a new batch prepared by identical procedures, while samples No. 4 and No. 5 were sintered together with the parallelepiped blocks, but in the shape of discs with a diameter of 25 mm and a thickness of 1.7 mm only for the dielectric measurements. The faces were made conducting with Ag paste. All the experiments are consistent with each other, so that only a few representative results are presented here.

The dielectric susceptibility $\chi(\omega,T) = \chi' - i\chi''$ was measured with an HP 4194 A impedance bridge with a four-wire probe and an electric field of 0.5 V/mm, between 0.1 and 100 kHz. The heating and cooling runs were made at 0.1–1.5 K/min in a Delta climatic chamber. The dynamic Young's modulus was measured in vacuum by electrostatically exciting the flexural modes of the bars suspended on thin thermocouple wires.[17] Below we present the reciprocal of the Young's modulus E, the compliance $s(\omega,T) = s' - is''$, the mechanical analog of the dielectric susceptibility, measured on the fundamental mode with $\omega/2\pi \sim 1.6$ kHz. Since $\omega \propto \sqrt{E'}$,[18] the temperature variation of s is given by $s(T)/s_0 \simeq \omega_0^2/\omega^2(T)$, where ω_0 is chosen so that s_0 represents the compliance in the paraelectric phase.

Powder x-ray diffraction was performed on a PANalytical X'Pert Pro MPD, utilizing Cu Kα_1 radiation ($\lambda = 1.540598$ Å) monochromated with a curved-Johansson premonochromator, and a PIXcel detector in Bragg-Brentano geometry. Variable temperature environmental control was performed using an Anton Paar HTK1200 furnace stage, and diffraction patterns covering the range $2\theta = 15°$ to 90° were collected for ~140 min at fixed temperatures reached with ramps of 1–2 K/min, so that the average temperature rate was 0.065 K/min below 363 K and 0.013 K/min above that temperature. Phase fractions were refined using the Rietveld method as implemented in TOPAS Academic, wherein only the lattice parameters and peak shapes of the two independent *Pbam* and *R*3*m* phases were allowed to refine. The atomic coordinates of the two structures were fixed in order to reduce the number of refining parameters.[19]

III. RESULTS

Figure 1 presents the fraction of the *Pbam* O-AFE phase deduced from XRD, the dielectric susceptibility χ' and elastic compliance s' measured during slow cycling between room temperature and ~ 400 K with cooling rates $\leqslant 0.1$ K/min. The corresponding heating ramps of the anelastic and dielectric experiments were at $\leqslant 0.4$ and 1 K/min, respectively, but the temperature rate has little influence during heating (see Discussion and Fig. 2). The upper temperatures reached during these cycles differ slightly from each other, but the numerous experiments we carried out show that the upper temperature has little influence on the shape and position of the anomalies, even if T_C is exceeded; what is affected is the background level,

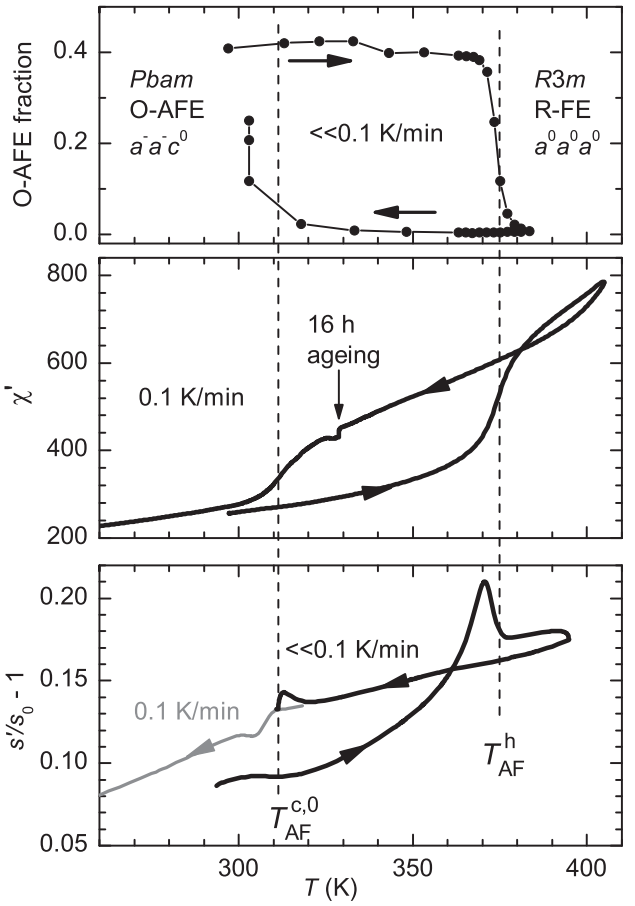

FIG. 1. Fraction f_{AF} of the *Pbam* phase, real part of the dielectric susceptibility χ', and of the elastic compliance s' measured during slow cycling at the rates indicated in the labels.

which corresponds to the tail of the Curie-Weiss peak with an important contribution from ferroelectric domain walls.

The XRD and dielectric methods clearly identify the transitions between then O-AFE and R-FE phases at $T^h_{AF} = 375$ K during heating and $T^{c,0}_{AF} = 311$ K during cooling, from the middle of the steps in $\chi'(T)$. For a definition of all the characteristic temperatures used in the article and the type of the associated elastic anomalies see Table I. The superscript 0 stands for a quasistatic experiment, in practice at a cooling rate $\leqslant 0.1$ K/min. Even though the loop of the χ' curves on cooling and heating is closed, the transition to the *Pbam* phase may be largely incomplete. In fact, according to XRD there is a substantial fraction of the R-FE phase down to room temperature, which is slightly below T^c_{AF}. This indicates that the transformation to the *Pbam* phase is sluggish, and its actual completion occurs at lower temperature or requires a very long time.

The elastic compliance also has anomalies at the same temperatures deduced from the other two methods, but their shape may change between heating and cooling and the hysteresis is not closed. The elastic anomalies consist of peaked and step components that can combine differently depending on the temperature rate (see also the following figures). The black cooling curve is the slowest run, whose

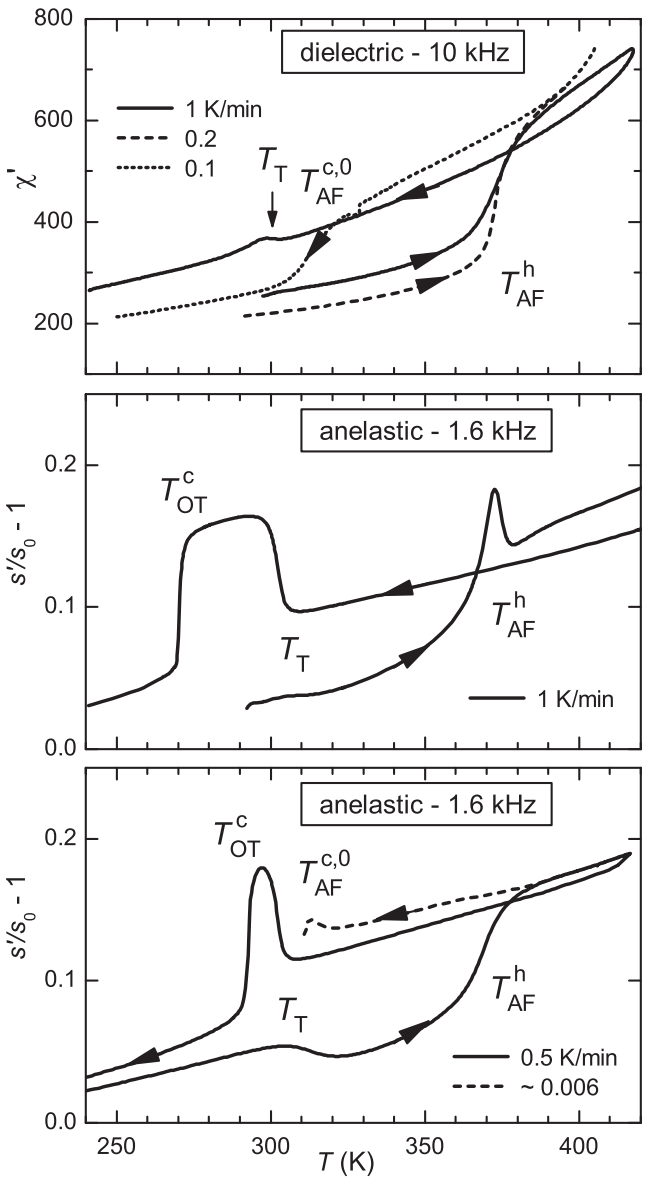

FIG. 2. Dielectric susceptibility χ' and elastic compliance s' measured during temperature cycling with the indicated cooling rates.

final 5 K were measured in 14 h (∼6 mK/min), resulting in a sharpening and shift to higher temperature of the anomalies with respect to the usual runs. The quasistatic cooling was stopped when the onset of the downward step (stiffening indicating $T_{OT}^{c,0}$; see later on) was evident; at this point temperature was raised to 318 K and cooling was restarted at a faster rate of 0.1 K/min (gray curve), so that the progress of the transformations extended to a lower and broader temperature range. These observations confirm that the kinetics of the transformation is very slow during cooling, although not relevant above ∼330 K. In fact, 16 h ageing at 329 K only produces a small dip in χ' at that temperature, with no further consequence when the slow cooling is restarted.

Figure 2 further demonstrates that the $R3m \rightarrow Pbam$ transition is sluggish during cooling through T_{AF}^{c}, such that it is unobservable in χ' measured at −1 K/min, while kinetic effects are far less important during heating through the considerably higher temperature T_{AF}^{h}. In fact, in the two χ' curves measured during heating at 0.2 and 1 K/min, the anomaly at T_{AF}^{h} has the same temperature and width (the same is true at least up to 1.5 K/min; not shown here), while the different backgrounds may be attributed to different aging conditions and hence different extrinsic contribution from domain wall relaxation.

Figure 2 also shows that the $Pbam \leftrightarrow R3m$ transition is actually split into two components with different kinetics, one of which is clearly seen only as a sharp steplike stiffening (decrease of s) during cooling at a temperature indicated as T_{OT}^{c}, which is lower than but approaches T_{AF}^{c} when quasistatic conditions are approached. This transition must involve a nonpolar mode, since it is visible in the elastic but not in the dielectric response, and the most obvious attribution is to the condensation of the $a^-a^-c^0$ tilt mode of the orthorhombic phase, denoted OT for brevity. In addition, the $s(T)$ curves during heating exhibit different shapes, but the anomalies connected with the $Pbam \leftrightarrow R3m$ transition occur at nearly the same temperatures $T_{OT}^{h} \simeq T_{AF}^{h}$. In addition to these anomalies, a clear step is visible at T_T during cooling, with a small thermal hysteresis and attenuated during heating. A small effect is found also in $\chi(T)$ at the same T_T, when cooling is so fast to hinder the formation of the $Pbam$ phase.

IV. DISCUSSION

As anticipated in Introduction, the observations of large thermal hysteresis and slow kinetics of nucleation of the AFE phase in PZT are not new. Dielectric curves similar to those shown here have been reported for variously doped PZT[7–9] and $Pb_{1-x}Ba_xZrO_3$,[10,11] where also the fractions of AFE and FE phases were monitored by XRD,[12] as in Fig. 1. Such phenomena are supposed to involve the stabilization

TABLE I. Transition temperatures with meaning, phases that they separate, and effect on the compliance during cooling. Superscript h/c = heating/cooling; superscript 0 = quasistatic; L/SRO = long-/short-range order. A softening (steplike increase) during cooling becomes a hardening during heating and *vice versa*. The transition at T_{IT} is explained at the end of Discussion; it is assumed that at 5% Ti it is $T_{IT} = T_C$ and therefore the $R3m$ phase is tilted with SRO.

Temperature	Meaning	Phases	s' anomaly on cooling
T_C	Curie temperature	FE ↔ PE	Peak
T_T	Tilting (LRO $a^-a^-a^-$)	$R3c \leftrightarrow R3m$ (untilted or SRO tilted)	Softening
T_{AF}	AFE ↔ FE (cation displacements)	$Pbam \leftrightarrow R3m$	Softening
T_{OT}	Orthorhombic tilt (LRO $a^-a^-c^0$)	$Pbam \leftrightarrow R3m$	Hardening
T_{IT}	Intermediate tilt = SRO tilting	$R3m$ SRO tilted ↔ $R3m$ untilted	Broad softening

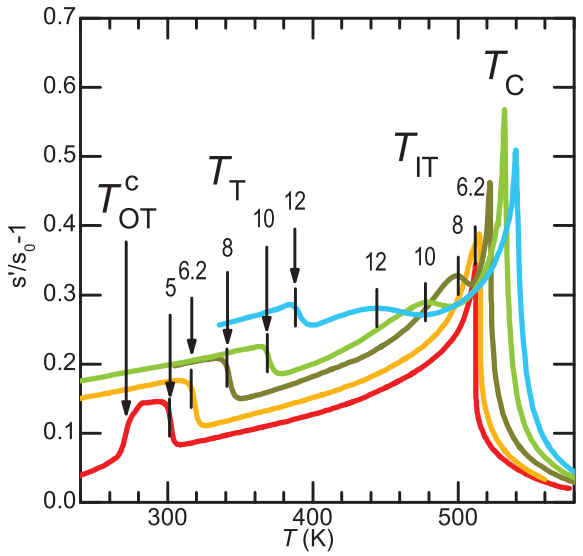

FIG. 3. (Color online) Elastic compliance s' measured during cooling on samples with $x \geqslant 0.05$. The tilt transition temperatures are indicated with vertical bars and arrows (the curves for $x > 0.05$ from Refs. 16,20).

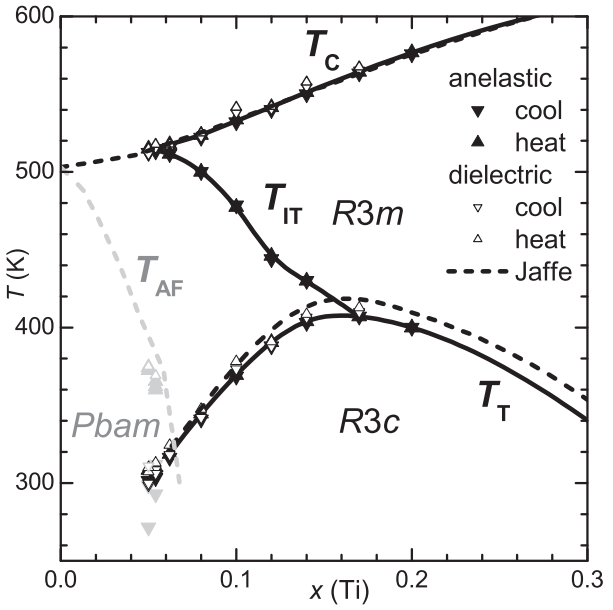

FIG. 4. Zr-rich region of the phase diagram of PZT. The dashed lines are from the accepted phase diagram;[23] the points and continuous lines are our revisions from Ref. 20. The points of T_{AF} are indicated in gray to avoid confusion with T_T. The transition at T_{IT} is explained at the end of Discussion.

of the FE phase by charged defects arising from doping, off-stoichiometry, but also from microcracking during the AFE/FE transition itself, at least for $Pb_{1-x}Ba_xZrO_3$.[10]

Even in light of the above observations, the behavior of the χ and especially the s curves measured under different conditions in Results may appear at first puzzling. It can be explained as follows, by considering separately the polar and AFD components of the transition to the O-AFE phase. The transition to the *Pbam* phase is very sluggish, and therefore one has coexistence with the *R*3*m* phase. On the other hand, the *R*3*m* fraction still undergoes the transition to the $a^-a^-a^-$ tilted *R*3*c* phase below a temperature T_T, as found at higher Ti content.[16,20] From the sequence of s curves at increasing Ti composition in Fig. 3, it is clear that s for $x = 0.05$ has the same step at T_T plus an additional transition at T^c_{OT}. Moreover, Fig. 4 shows that T_T of $x = 0.05$ is exactly the extrapolation of the $T_T(x)$ border to long-range $a^-a^-a^-$ tilting.[16,20] At least down to $x = 0.05$, the T_T line falls within the range of the AFE thermal hysteresis, whose lower limit during normal or fast cooling is below the temperature scale of the figure. The T_T transition is rather sharp and occurs at the stable temperatures $T^c_T = 301$ K and $T^h_T = 310$ K during cooling and heating, respectively. The step during heating is always smaller because the fraction f_{AF} of O-AFE phase increases while being kept at low temperature, but is observable even after cycling down to 100 K or waiting for weeks at room temperature. The concomitant occurrence of dielectric anomalies at T_T and T_{AF} had already been noted in $PbZr_{0.95}Ti_{0.05}O_3$ with various levels of Nb doping.[7]

The transformation to the *Pbam* phase involves two separate modes with different kinetics. One is the sluggish polar mode visible in the dielectric susceptibility only for sufficiently slow cooling. This must correspond to the establishment of the AFE displacements of the Pb atoms along ⟨110⟩ with a period of four pseudocubic unit cells,[21,22] and therefore we call it the AFE mode and its temperature T_{AF}. The other mode must be the nonpolar remaining ingredient of the *Pbam* phase, and therefore the mode that gives rise to the $a^-a^-c^0$ tilt pattern. Its temperature T^c_{OT} approaches $T^{c,0}_{AF}$ in a quasistatic experiment, but can be considerably decreased at rates > 0.1 K/min. From Figs. 1 and 2 it turns out that $T^c_{OT} \simeq T^{c,0}_{AF} = 311$ K at ~ 0.006 K/min, 307 K at 0.1 K/min, 293 K at 0.5 K/min and 270 K at 1 K/min. It is remarkable that a faster cooling rate results in a lower T^c_{OT} but the step remains sharp. This suggests that the OT mode collapses abruptly once the AFE mode has frozen over a critical volume fraction and/or correlation length.

During quasistatic cooling, as seen in XRD, the temperatures of the two components AFE-FE and OT are maximal and coincide. During heating, thanks to the large thermal hysteresis, the kinetics are not critical, and both transitions are almost coincident at $T^h_{AF} \simeq 375$ K, but still can be distinguished in the $s(T)$ curves.

The effect of the three transitions on the compliance is well reproduced by three independent steps $\Delta s^{(x)}(T)/s_0 = f_x s_x [1 - \tanh((T - T_x)/\Delta T_x)]/2$ of amplitudes s_x and centered at the temperatures $T^{h|c}_x$ with widths $\Delta T^{h|c}_x$, where $x =$ T, OT and AF stand for tilt (within the R domains), orthorhombic tilt, and AFE modes. In the minimal model there is no concern for possible intermediate steps of the AFE transition within which the OT tilting occurs, and only one independent fraction f_{AF} is introduced. The fraction that transforms into O-AFE is $f_{AF} = f_{OT}$, and it is assumed that T_T is from the remaining fraction $1 - f_{AF}$, with f_{AF} changing between heating and cooling, but constant over the whole temperature range of each curve. In this manner it is possible to reproduce the

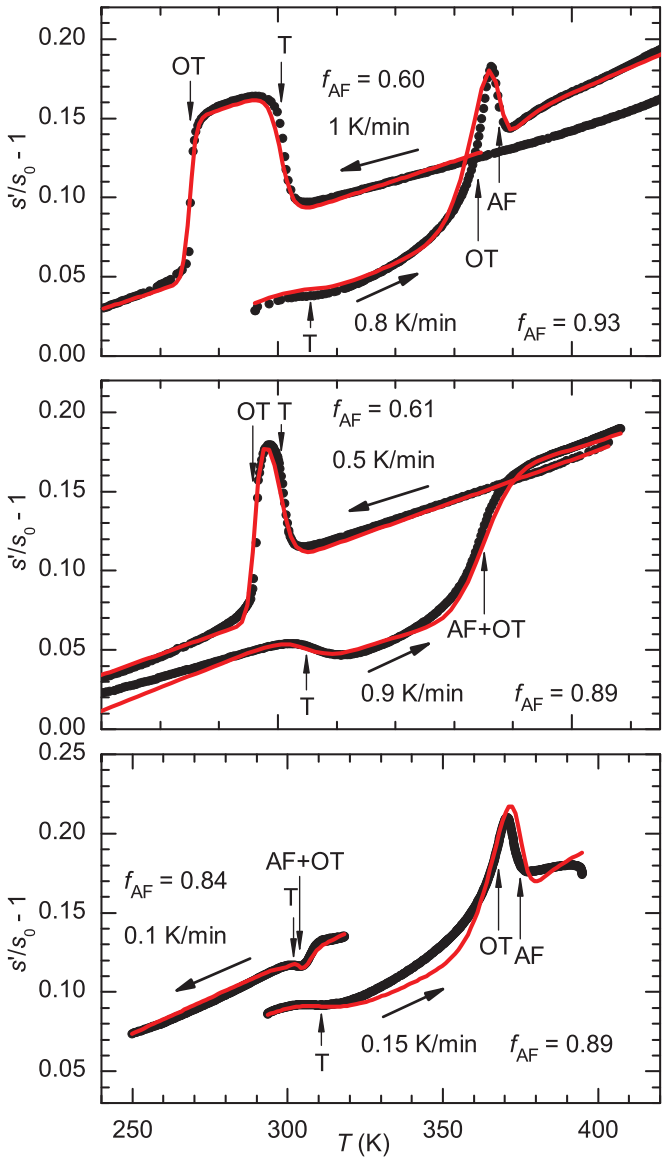

FIG. 5. (Color online) Reciprocal Young's modulus measured on sample No. 3 under different initial conditions and temperature rates indicated in the figure. The continuous lines are fits with steplike anomalies with the temperatures indicated by arrows and the same amplitudes, as described in the text. For clarity, the transition temperatures $T_x^{h|c}$ are labeled only with x, and cooling/heating are distinguished by arrows.

compliance curves measured under all conditions however different they appear from each other. Figure 5 presents three representative cases fitted with almost the same amplitudes $s_T = 0.214 \pm 0.013$, $s_{OT} = -0.176 \pm 0.016$, $s_{AF} = 0.12$. The errors represent the variation between the first two cases, with identical values, and the third case of much slower rates; the adjustment is anyway small and might be reduced by further refinements of the fits (the main oversimplifications are the assumptions of linear backgrounds and of constant f_{AF} during cooling). The other parameters are $T_T^c = 301.5 \pm 0.5$ K, $\Delta T_T^c = 4.3$ K, $T_T^h = 310.5 \pm 0.5$ K, $\Delta T_T^h = 10 \pm 1$ K, $T_{AF}^h = 372.5 \pm 2.5$ K, $T_{OT}^h = 369 \pm 1$ K, while T_{OT}^c, $T_{AF}^c \leqslant 304$ K vary considerably depending on the cooling rate; in the first two cases it is assumed that T_{AF}^c is below the lowest temperature attained, while all the other T_x are indicated by arrows. The maximum fractions f_{AF} of O-AFE phase are reported in the figure. The fraction of transformed AFE phase on heating is 89%–93%, higher than the maximum fraction found by XRD, but this is attributable to the lower minimum temperatures reached during cycling.

An interesting feature of the transition at T_{OT}^c is that it consists of a steplike stiffening, opposite to the softening at T_T^c in the $R3c$ phase. The latter behavior is the usual one, and is predicted when a strain ε is coupled with the square of the order parameter Q^2, which is the case for shear strains with the tilt angles of the octahedra. Actually, the situation is more complicated and requires an analysis of the complete expressions of the anomalies in the elastic constants at various tilt transitions in terms of the coefficients of the Landau expansion of the free energy.[24] Such expressions define steplike softenings, though for some of the shear constants they may in principle have the opposite sign. We are not aware of any analysis of the parameter space defining regions where such constants would undergo stiffening, but in practice the usual case is softening. This is especially true for the Young's modulus of polycrystals, which contains the contribution from all the elastic constants that certainly undergo softening. Lacking a detailed analysis, we cannot exclude the possibility that the $a^-a^-c^0$ tilting of the $Pbam$ phase produces a stiffening of the Young's modulus when coming from an untilted phase, but we advance another explanation: the transition is between two differently tilted phases with the loss of a tilting axis. In fact, in addition to that at T_T, another softening is observed at a temperature T_{IT} that starts from the $T_T(x)$ line at its maximum at $x \simeq 0.15$ and merges with $T_C(x)$ at $x \simeq 0.06$.[4,16] We interpret such an anomaly as an initial stage of short-range ordered octahedral tilting, and propose that the same disordered tilting occurs also for $x < 0.06$ concomitantly with the FE transition at T_C.[4] According to this interpretation, at $x = 0.05$ the phase normally labeled $R3m$ has this space group symmetry only on average, but is locally tilted below T_{IT}. Extending Glazer's notation, the tilt system would be $a^*a^*a^*$, where the asterisks denotes that there is neither in-phase nor antiphase correlation along the axis.[4] Then the transition to the long-range ordered $a^-a^-c^0$ tilt system would involve the loss of tilting about the c axis, making the occurrence of stiffening reasonable. In addition, first-principle calculations indicate that the $R3m$ phase of PZT with $x = 0.05$ is strongly unstable against octahedral tilting, and the apparent contradiction with the diffraction experiments was solved by supposing that the tilts are disordered.[25]

V. CONCLUSIONS

The phase transformations of $PbZr_{0.95}Ti_{0.05}O_3$ present a complex phenomenology depending on thermal history and rate, as a result of the energetic equivalence of the orthorhombic AFE $Pbam$ phase, the ground state of $PbZrO_3$, and the rhombohedral FE phases with their tilted and untilted variants $R3c$ and $R3m$. The determination of the $Pbam$ fraction during quasistatic temperature cycling has been complemented by measurements of the dielectric susceptibility χ and elastic

compliance s at varying temperature rates. Not only is the $R3m \rightarrow Pbam$ transition during cooling very slow, but it is also split into two distinct transitions: the slowest is a steplike decrease of both the dielectric and elastic susceptibilities and is interpreted as a polar FE-AFE mode, while a steplike increase visible only in the elastic compliance is interpreted as the antiferrodistortive tilt component. These transitions coincide during quasistatic cycling and during heating, where they occur at considerably higher temperature and faster rate. The coincidence of the temperatures for $a^-a^-c^0$ tilt order and AFE order to form the $Pbam$ phase during quasistatic cycling is ascribable to coupling between the two modes, which, however, are subjected to different driving forces and have different kinetics.

ACKNOWLEDGMENTS

The authors thank C. Capiani (ISTEC) for the skillful preparation of the samples, and P. M. Latino (ISC) and R. Scaccia (ISC) for their technical assistance in the anelastic and dielectric experiments. D.S.K. thanks the Science City Research Alliance and the HEFCE Strategic Development Fund for financial support. The PANalytical MPD diffractometer used in this research was obtained through the Science City Energy Futures Project, Hydrogen Energy, with support from Advantage West Midlands (AWM). F.C., F.C., and C.G. acknowledge partial support from European COST Action SIMUFER MP0904 "Single and multiphase ferroics and multiferroics with restricted geometries."

[1] E. Sawaguchi, J. Phys. Soc. Jpn. **8**, 615 (1953).
[2] A. Amin, R. E. Newnham, L. E. Cross, and D. E. Cox, J. Sol. State Chem. **37**, 248 (1981).
[3] I. A. Kornev and L. Bellaiche, Phys. Rev. B **79**, 100105 (2009).
[4] F. Cordero, F. Craciun, F. Trequattrini, and C. Galassi, Phase Trans. (2013), doi: 10.1080/01411594.2013.796590.
[5] N. Zhang, H. Yokota, A. M. Glazer, and P. A. Thomas, Acta Cryst. B **67**, 461 (2011).
[6] J. Ricote, D. L. Corker, R. W. Whatmore, S. A. Impey, A. M. Glazer, J. Dec, and K. Roleder, J. Phys.: Condens. Matter **10**, 1767 (1998).
[7] J. Handerek and Z. Ujma, J. Phys.: Condens. Matter **7**, 1721 (1995).
[8] M. Avdeev, J. D. Jorgensen, S. Short, G. A. Samara, E. L. Venturini, P. Yang, and B. Morosin, Phys. Rev. B **73**, 064105 (2006).
[9] Z. Xu, X. Dai, and D. Viehland, Phys. Rev. B **51**, 6261 (1995).
[10] B. P. Pokharel and D. Pandey, J. Appl. Phys. **86**, 3327 (1999).
[11] B. P. Pokharel and D. Pandey, J. Appl. Phys. **88**, 5364 (2000).
[12] B. P. Pokharel and D. Pandey, J. Appl. Phys. **90**, 2985 (2001).
[13] K. Roleder and J. Dec, J. Phys.: Condens. Matter **1**, 1503 (1989).
[14] J.-H. Ko, M. Górny, A. Majchrowski, K. Roleder, and A. Bussmann-Holder, Phys. Rev. B **87**, 184110 (2013).
[15] F. Cordero, F. Craciun, and C. Galassi, Phys. Rev. Lett. **98**, 255701 (2007).
[16] F. Cordero, F. Trequattrini, F. Craciun, and C. Galassi, J. Phys.: Condens. Matter **23**, 415901 (2011).
[17] F. Cordero, L. Dalla Bella, F. Corvasce, P. M. Latino, and A. Morbidini, Meas. Sci. Technol. **20**, 015702 (2009).
[18] A. S. Nowick and B. S. Berry, *Anelastic Relaxation in Crystalline Solids* (Academic Press, New York, 1972).
[19] See Supplemental Material at http://link.aps.org/supplemental/10.1103/PhysRevB.88.094107 for the Rietveld refinements.
[20] F. Cordero, F. Trequattrini, F. Craciun, and C. Galassi, Phys. Rev. B **87**, 094108 (2013).
[21] F. Jona, G. Shirane, F. Mazzi, and R. Pepinsky, Phys. Rev. **105**, 849 (1957).
[22] D. L. Corker, A. M. Glazer, J. Dec, K. Roleder, and R. W. Whatmore, Acta Cryst. B **53**, 135 (1997).
[23] B. Jaffe, W. R. Cook, and H. Jaffe, *Piezoelectric Ceramics* (Academic Press, London, 1971).
[24] R. A. McKnight, C. J. Howard, and M. A. Carpenter, J. Phys.: Condens. Matter **21**, 015901 (2009).
[25] K. Leung, E. Cockayne, and A. F. Wright, Phys. Rev. B **65**, 214111 (2002).